Proceedings of ASME Turbo Expo 2011
GT2011
June 6-10, 2011, Vancouver, British Columbia, Canada

GT2011-45926

EFFECT OF RIB SPACING ON HEAT TRANSFER IN A TWO PASS RECTANGULAR CHANNEL (AR=2:1) AT HIGH ROTATION NUMBERS

Jiang Lei and Je-Chin Han
Texas A&M University
College Station, Texas, USA
Email: jc-han@tamu.edu

Michael Huh
The University of Texas at Tyler
Tyler, Texas, USA
Email: mhuh@slb.com

ABSTRACT

In this paper the effect of rib spacing on heat transfer in a rotating two-passage channel (*AR*=2:1) at orientation angle of 135° was studied. Parallel ribs were applied on leading and trailing walls of the rotating channel at the flow angle of 45°. The rib-height-to-hydraulic diameter ratio (e/D_h) was 0.098. The rib-pitch-to-rib-height (*P/e*) ratios studied were 5, 7.5, and 10. For each rib-spacing, tests were taken at five Reynolds numbers from 10,000 to 40,000 and for each Reynolds number, experiments were conducted at four rotational speeds up to 400 rpm. Results show that the heat transfer enhancement increases with decreasing *P/e* from 10 to 5 under non-rotation condition. However, the effect of rotation on the heat transfer enhancement remains about the same for varying *P/e* from 10 to 5. Heat transfer enhancement due to rotation can be correlated on all surfaces (leading, trailing, inner and outer walls and tip cap region) in the two-passage 2:1 aspect ratio channel.

INTRODUCTION

Various cooling techniques have been invented and applied in gas turbines to prevent the detrimental problems. Many of these techniques are summarized and discussed in Han et al. [1]. One of the cooling techniques is the application of turbulators (trip strips) on the internal surfaces of pressure side and suction side of gas turbine blades. It is seen in Figure 1 that the cross section of the internal channel varies according to the thickness of the blade from the leading edge to trailing edge. For the simplified facilities used in laboratory experiments, rectangular channels are used to model the gas turbine blade internal cooling passages. The aspect ratio (*AR*) of the rectangular channel is defined as the ratio of the width (*W*) to the height (*H*) and determined by the relative location of the channel. Near the leading edge portion, a channel of the smallest *AR*=1:4 is used and in the mid portion channels of *AR*=1:2, 1:1, and 2:1 are applied and near trailing edge, a channel of largest *AR*=4:1 is used to simulate those in real gas turbines.

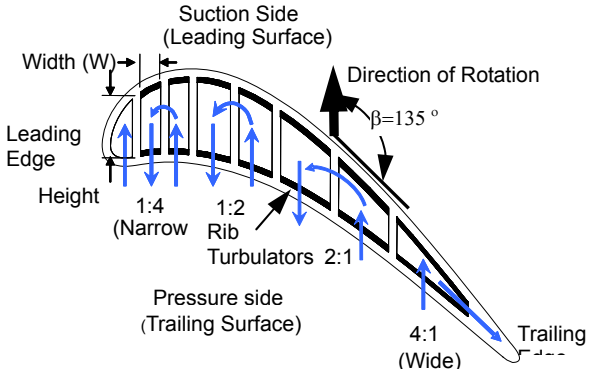

Fig. 1 Gas turbine internal cooling passages

ASPECT RATIO EFFECTS (STATIONARY)

A number of previous studies have shown that the aspect ratio of the channel plays an important role in the heat transfer and flow field at stationary condition. Han [2] studied the effect of aspect ratio on heat transfer for five different channels (*AR*=1:4, 1:2, 1:1, 2:1, and 4:1) at two rib pitch to height ratios (*P/e*=10 and 20). A correlation based on heat transfer and friction coefficient was developed for ribbed channels covering aspect ratio, rib spacing, rib height, and Reynolds number. Han and Park [3] investigated the combined effects of rib flow-angle (α=30°, 45°, 60°, and 90°) and channel aspect ratio (*AR*=1:1, 2:1, and 4:1). The rib flow-angle was successfully absorbed into the correlation. Park et al. [4] studied the combined effects of channel aspect ratio (*AR*=1:4, 1:2, 1:1, 2:1, and 4:1), rib flow-angle (α=30°, 45°, 60°, and 90°) and Reynolds number on heat transfer and pressure drop. The results suggest that the narrow channels (*AR*=1:4 and 1:2) give better heat transfer performance than wide ones (*AR*=2:1 and 4:1). 60°/45° angled ribs are recommended for square channel,

45°/60° angled ribs for narrow channels and 30°/45° angled ribs for wide channels.

RIB SPACING EFFECTS (STATIONARY)

The rib spacing in the internal cooling passage is very important to heat transfer and pressure drop. Too large spacing can result in reduction of the heat transfer enhancement brought by ribs. Too small spacing can induce large pressure drop. Han et al. [5] studied the effect of rib shape, attack angle (α) and rib pitch-to-height ratio (P/e) on heat transfer and friction coefficient in a narrow ribbed channel (AR=12:1). As P/e ratio varies from 5 to 7.5, 10, 15, and 20, both friction factor and Stanton number increase at first and then decrease with the maximum value occur at P/e=10. Taslim and Spring [6] applied liquid crystal technique to investigate the effects of rib profile and rib pitch-to-height ratio (P/e) in a rectangular 2:1 channel. Their results showed that the for given rib profile and blockage ratio (e/D_h), an optimum rib pitch-to-height ratio (P/e) existed.

ROTATION NUMBER EFFECTS

In real turbines, rotation of blades affects the heat transfer in the cooling passage. Wagner et al. [7, 8] provided sets of data in a smooth square multi-passage channel with rotation number ranged from 0.0 to 0.48. They concluded that the local heat transfer coefficients decrease up to 60 percent on the leading surface and increase 250 percent on the trailing surface from the non-rotation levels in the first passage. Han et al. [9] studied the influence of uneven wall temperature in a two-pass smooth square channel. The results suggested that the effect of uneven wall temperatures in the second-pass radially inward flow is greater than that in the first-pass radially outward flow. Huh [10] studied the rotation effect on heat transfer in a two-pass smooth rectangular channel (AR=2:1) with developing entrance flow. The rotation number ranged from 0.0 to 0.45. Results showed that heat transfer was highly increased in the sharp 180° turn portion.

Wagner et al. [11] extended his work from smooth to ribbed-roughed channels using orthogonal ribs with P/e=10 and e/D_h=0.1. The overall heat transfer coefficient in the passage was almost doubled compared with the smooth case. Johnson et al. [12] studied the effects of 45° angled ribs and 45° channel orientation. Taslim et al. [13] performed an experiment studying the effect of rotation on heat transfer using liquid crystal technique in criss-cross ribbed channel with P/e=10 and e/D_h=0.133, 0.250, and 0.333.

Fu et al. [14, 15] performed experiments in an unpressurized test section for five different ribbed channels (AR=1:4, 1:2, 1:1, 2:1, and 4:1). The rotation number varied from 0 to 0.3. Su et al. [16] reported his CFD results on rotating channels with AR=1:1, 1:2, and 1:4. The rotation number ranged from 0.0 to 0.28. Their results showed that for large Reynolds numbers, the effect of rotation decreases with a decrease in aspect ratio.

Liu et al. [17] studied the effect of angled rib spacing in a rotating channel with AR=1:2. The rotation ranged from 0.0 to 0.2. The results showed that the P/e=3 case had the best heat transfer performance and the effect of rotation was increased as angled rib spacing decreased. Huh et al. [18] studied the effect of angled rib spacing in a rotating channel with AR=1:4. The rotation number varied from 0.0 to 0.65. The results showed that the P/e=2.5 case had the highest heat transfer enhancement.

CHANNEL ORIENTATION EFFECTS

Johnson et al. [19] conducted experiments in rotating smooth and ribbed multi-pass square channels with orientation angle 0°and 45°. On the leading surface of the first pass, the heat transfer of 45° orientation case was almost twice and the effects of Coriolis and buoyancy forces were reduced comparing to 0° orientation case. Parsons et al. [20] performed experiments to study the effect of channel orientation and wall heating condition in a two-pass ribbed square channel. Dutta and Han [21] studied heat transfer in a two-pass smooth square channel with an orientation angle of 0°, 45° and 90°. Nusselt number ratios vary with the channel orientation angle. Azad et al. [22] performed heat transfer experiments in a rotating two-pass rectangular ribbed channel with AR=2:1 and P/e=10 for orientation angles of 90° and 135° with maximum rotation number of 0.21. Al-Hadhrami et al. [23] obtained heat transfer data for the two-pass rectangular channel (AR=2:1) with two channel orientations of 90° and 135° using 45° V-shaped ribs. They concluded that 90° orientation channel produced higher heat transfer over 135° orientation. Huh et al. [24] conducted heat transfer experiments in a rotating two-pass rectangular channel with AR=2:1 for two channel orientations 90° and 135° using smooth and ribbed surfaces. The rotation number and buoyancy parameter reached 0.45 and 0.85 respectively. It was observed that the channel orientation was important and beneficial to heat transfer augment on leading surface in the first pass at high rotation numbers.

OBJECTIVES

From the review of previous work, it is clear that many parameters can influence the heat transfer in the gas turbine blade cooling passage. Up to this point, only limited research has been presented for rotating two-pass rectangular channels (AR=2:1) with ribbed walls. Azad et al. [22] and Al-Hadhrami et al. [23] showed data for an AR=2:1 ribbed two-pass channel with 135° passage orientation and fully-developed flow for rotation number (Ro) limited to 0.21 (at lower Re=5,000), only one pitch-to-height ratio (P/e=10), and no tip cap region data provided. This study aims to present a complete set of heat transfer data for the AR=2:1 ribbed two-pass channel with 135° passage orientation at large rotation numbers and with a developing entrance flow. The objectives of the current study are as follows:

1. Investigate the effects of rib pitch-to-height ratio (P/e) on heat transfer in a two-pass 2:1 aspect ratio channel with

45° parallel ribs considering smooth case and three pitch-to-height ratios: P/e=5, 7.5, and 10 at the passage orientation 135°.
2. Determine the effects of rotation and buoyancy on all surfaces (leading, trailing, inner and outer walls, and tip cap region) of the 2:1 aspect ratio channel.
3. Develop correlations to predict the heat transfer enhancement due to rotation on all walls (leading, trailing, inner and outer walls, and tip cap regions) of the two-pass 2:1 aspect ratio channel.
4. Extend the rotation number and buoyancy parameter in the ribbed 2:1 aspect ratio channel with an orientation of 135° to 0.45 and 0.8 respectively, which is more than four times of previous studies in the 2:1 aspect ratio channel.

NOMENCLATURE

A_p	copper plate projection area
A_{htr}	heater surface area
AR	aspect ratio
Bo_x	local buoyancy parameter
c_p	specific heat at constant pressure
D_h	hydraulic diameter
e	rib height
H	channel height
h	regionally averaged heat transfer coefficient
i	designates a given region in the channel ($1 \le i \le 12$)
I	current
k	thermal conductivity of the air
m	mass flow rate
Nu	regionally averaged Nusselt number
Nu_o	Nusslet number for a fully-developed flow in a stationary smooth pipe
Nu_s	stationary regionally averaged Nusselt number
P	rib pitch
Pr	Prandtl number of the air
Q_n	net heat transfer rate
Q_l	external heat loss rate
R_x	local radius of rotation
$\overline{R}$	mean radius of rotation
Re	Reynolds number
Ro	Rotation number, $\Omega D_h/U_b$
$T_{w,x}$	regionally averaged wall temperature
$T_{b,x}$	local coolant bulk temperature
$T_{f,x}$	local film temperature
U_b	velocity in streamwise direction
V	voltage
W	channel width
α	rib flow angle
β	channel orientation angle to the axis of rotation
μ	dynamic viscosity of coolant
$\rho_{b,x}$	local air density based on local bulk temperature
$\rho_{w,x}$	local air density based on local wall temperature
$\Delta\rho/\rho_{b,x}$	local bulk-to-wall density ratio ($\Delta\rho=\rho_{b,x}-\rho_{w,x}$)
Ω	rotation speed

EXPERIMENT SETUP

For gas turbines in aircrafts, the typical rotation numbers reach 0.25 with Reynolds number of 25,000. High pressure air is used to achieve similar conditions for the large rotation number in the laboratory by increasing its density if temperature does not change much. For a fixed mass flow rate (Reynolds number) and hydraulic diameter, increasing density decreases velocity and in turn increases the rotation number. In order to achieve larger rotation numbers at higher Reynolds numbers, the experiments for the present study were conducted with air at a pressure of 68 psig. The Reynolds numbers tested in this study were 10000, 15000, 20000, 30000 and 40000. At each Reynolds number, the rotation speed varied from 0 to 400 rpm with an increment of 100 rpm.

ROTATING FACILITY

Figure 2 shows the rotating arm assembly used to conduct the experiments for the current study. A steel table is used as the support structure. A 25 hp electric motor is used to drive the shaft which spins the arm. Counterweights are used to balance the arm so that minimal vibrations are experienced during rotation. Air from a compressor enters an ASME square-edge orifice meter (not shown) where the mass flow rate is measured. Air enters the rotating assembly at the bottom of the shaft via a rotary union and then passes through the hub and goes into the bore of the arm. A rubber hose is used to direct the flow from the arm to the test section housing. After the air flows through the test section, it exits the pressure vessel. The hot exhaust air is then directed, by another rubber hose, to the slip ring. A ½-inch copper tube, which passes through the bore of the slip ring, is used to direct the air to the top2 rotary union. Steel pipe is connected to the top rotary union and a valve is used to adjust the back pressure of the system.

TEST SECTION (AR=2:1)

Figure 3 (a) shows that the test section consists of two passes. The flow in the first passage is radially outward, and after a sharp 180º turn, the flow in the second pass is radially inward. There are a total of twelve regions in the test section in streamwise direction as shown in Figure 3 (c). Each passage consists of six regions, except for inner walls, which have 5 regions as shown and labeled in Figure 3 (c). The hydraulic diameter of each passage is 16.9 mm. The overall length of each passage is 203.0 mm and the distance between rotation axis and center of test section is 660.4 mm. The heated channel length of each passage is 157.0 mm and the unheated entrance length is 46.0 mm. One thermocouple is placed at the inlet and exit respectively to measure the air temperature as it enters or leaves the test section.

Copper ribs with a square cross-section are pasted on leading and trailing walls of the first and second pass by a very thin layer of super glue. The rib height (e) is 1.59 mm and three ratios of the rib pitch to the rib height investigated in this paper are P/e=5, 7.5 and 10 respectively. The ribs are placed at a flow angle (α) of 45° to the mainstream flow and the ribs on leading

and trailing walls are parallel to each other. The configurations of *P/e* ratios and flow angle are shown in Figure 4.

The thickness of all copper plates is 3.175 mm. The copper plates on the leading and trailing walls are square in shape and measure 23.81 mm x 23.81 mm except for those in the turn regions (#6 & #7 on both leading and trailing surfaces) which measure 28.58 mm x 28.58 mm and fillet 6.35 mm at the inner corner. The outer and inner wall copper plates are rectangular and measure 23.81 mm x 12.70 mm. The tip copper plates (tip cap #6 & #7) are rectangular with dimensions of 29.37 mm x 12.70 mm. Blind holes, with a diameter of 1.59 mm, are drilled 1.59 mm deep on the backside of each copper plate. Thermocouples are placed inside of the blind holes of the copper plates and are affixed to the copper plates using highly conductive epoxy. Temperature measurements were made on all of the leading, trailing, outer, inner and tip cap copper plates. Thus, a total of 48 temperature measurements were made from copper plates. The channel orientation angle (β) in this research is 135° as shown in Figure 3 (b) to approximate the rotation of a cooling passage in a real turbine blade.

DATA REDUCTION

HEAT TRANSFER ENHANCEMENT

This study investigates the regionally averaged heat transfer coefficient (h) on the walls at various Reynolds number and rotation speeds from Newton's Law of Cooling given in Eq. (1).

$$h = \left(Q_n / A_p\right) \Big/ \left(T_{w,x} - T_{b,x}\right) \quad (1)$$

The net heat transfer rate (Q_n) at each copper plate is calculated as heat input minus heat loss:

$$Q_n = \left(V^2 / R\right)\left(A_p / A_{htr}\right) - Q_l \quad (2)$$

To get the heat input to a copper plate, the power output of the heater is multiplied by the ratio of the projected area (A_p) of each copper plate to the total heater area (A_{htr}) of each heater and a uniform heat flux by the heater is assumed. To determine the heat losses (Q_l) escaping from each copper plate during the experiment, two heat loss calibration tests are performed for each rotational speed (including stationary case) at lower and higher temperatures of copper plate than the experiment (65°C at copper plate #4 and #10) respectively. The actual heat loss of each copper plate during the experiment is then determined by interpolating the temperature of each copper plate between the two sets of heat loss data. During the heat loss calibration tests, an insulating material is placed inside of the flow channel to minimize natural convection and the wall temperature of each copper plate is maintained by supplying power to each heater with the variac transformers. The temperature of each copper plate and voltage input of each heater are recorded when the total power input to the test section reaches equilibrium with the environment.

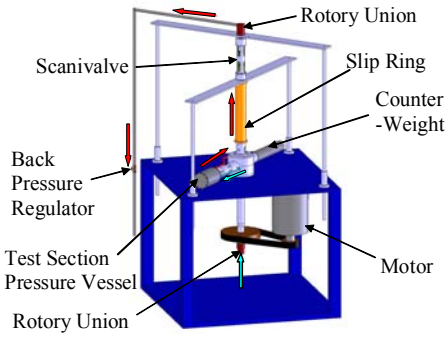

Fig.2 Rotating facility used to perform heat transfer experiment with 2X1 aspect ratio test section

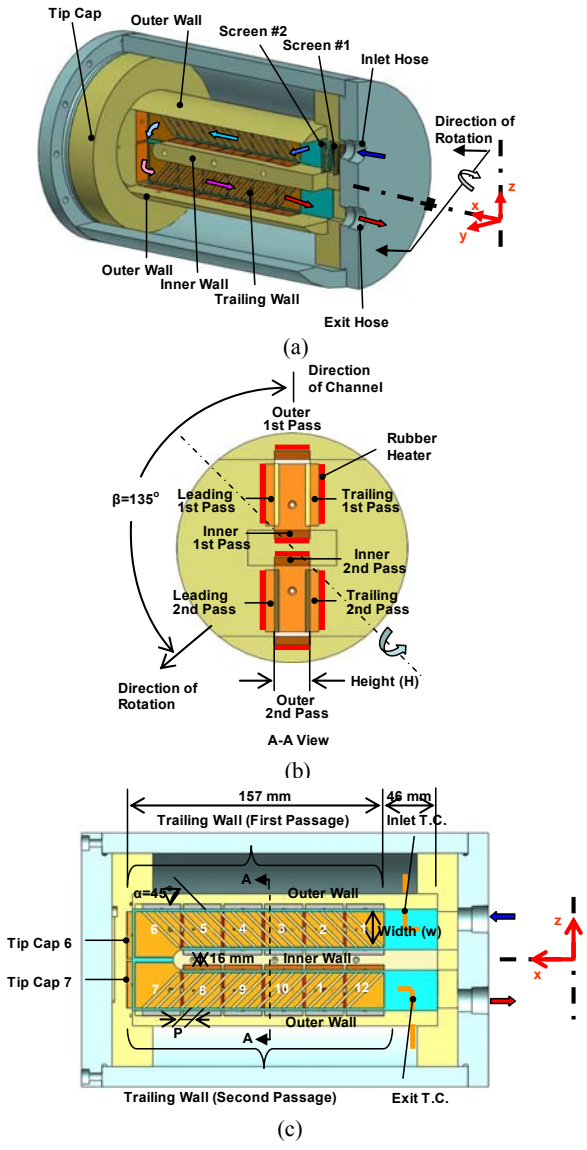

Fig. 3 (a) 3-D view of the 2X1 aspect ratio test section (b) Top view of the test section showing names of walls and corresponding heaters (c) Section view of the test section showing copper plate numbering

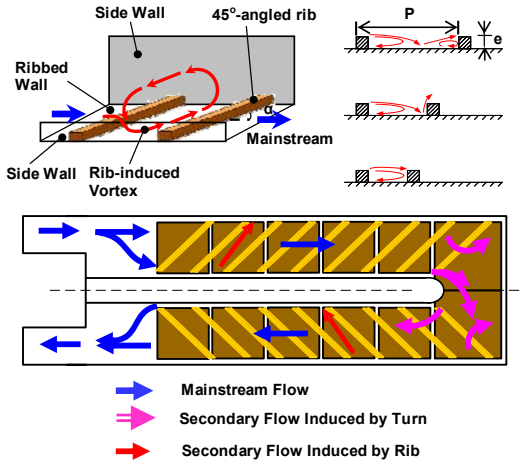

Fig. 4 Conceptual flow patterns around ribs and turn

The local regional wall temperature ($T_{w,x}$) is directly measured using the thermocouple installed in the blind hole on the backside of each copper plate. Because the plates are made of high-conductivity copper, the temperature of each plate is assumed uniform which has been proved in a separate test. One thermocouple at the inlet and another thermocouple at the outlet of the test section measure the inlet and outlet bulk temperatures, respectively. Therefore, the local bulk air temperature at any location in the test section can be calculated using linear interpolation. Another method to get the bulk temperature is by energy balance. The maximum difference of the outlet bulk temperatures by linear interpolation and energy balance is up to 10% at the lowest Reynolds number 10,000.

The Dittus-Boelter/McAdams correlation for heating ($T_{w,x} > T_{b,x}$) is used in this study to provide a basis of comparison. The Dittus-Boelter/McAdams correlation is used to calculate the Nusselt number (Nu_o) for fully developed turbulent flow through a smooth stationary pipe. Therefore, the heat transfer enhancement (Nu/Nu_o ratio) is given as:

$$(Nu/Nu_s)=[(h\cdot D_h)/k][1/(0.023\cdot Re^{0.8}\cdot Pr^{0.4}] \quad (3)$$

where heat transfer coefficient (h) is calculated by Eq. (1). All air properties are taken based on the channel average bulk air temperature with a Prandtl number (Pr) for air of 0.71.

EXPERIMENT UNCERTAINTY

An uncertainty analysis was performed based on the method described by Kline and McClintock [25]. The estimated uncertainty for the temperature instrumentation is 0.5°C. At lowest Reynolds number (Re=10,000), the maximum uncertainty of the Re is approximately 10% and the maximum uncertainty of the Nu is estimated as 12.5%.

DISCUSION OF RESULTS

FLOW FIELD BAHAVIOR

Figure 4 presents conceptual views of the most notable flow characteristics in ribbed channels. As the mainstream flow near the wall of the channel passes over the rib, it separates from the wall due to the rib, resulting in relatively low heat transfer downstream of the rib. However, when the mainstream flow reattaches to the wall (between two ribs), this is an area of relatively high heat transfer due to impingement of the relatively cool mainstream flow on the surface. Redevelopment of the boundary layer then begins. This pattern of separation, recirculation, and reattachment continues throughout the channel along with the pattern of repeating ribs. In addition, the rib turbulators increase turbulent mixing, which serves to increase the heat transfer from the channel wall.

The orientation of the rib turbulators has a significant impact on heat transfer by the previous observation that angled ribs yield higher heat transfer enhancement than orthogonal ribs due to the additional secondary flow. The fluid near the surface follows the angle of the rib from one side to the other in the passage creating a set of counter-rotating vortices, until it impinges on the side wall and returns through central portion of the channel as shown in Figure 4.

The ratio of rib pitch (P) to rib height (e) is also important. In Figure 4, for the largest P/e ratio case, flow passes the first rib and then separates forming a recirculation zone right after the first rib. It then reattaches the wall between the ribs and new boundary layer is redeveloped. For the medium P/e ratio case, flow separates and reattaches after passing the first rib, however, the redevelopment of the boundary layer is interrupted by the second rib. For the smallest P/e ratio case, flow separates and forms a recirculation zone after passing the first rib, however it can not reattach to the wall due to the very small distance between ribs. It can be expected that heat transfer is also highly affected by these flow patterns around ribs.

The entrance condition applied in this experiment affects the behavior of flow and heat transfer prominently and makes it different from the fully-developed cases by many other studies. Wright et al. [26] studied heat transfer in rectangular channels with aspect ratios of 4:1 and 8:1 for three different entrance geometries and concluded that the entrance effects will greatly enhance the heat transfer. Liu et al. [27] investigated heat transfer in a rotating channel with aspect ratio of 1:4 at high rotation numbers up to 0.65 for re-directed sharp bend entrance condition and showed the entrance condition reduced the effect of rotation in the first pass. Huh et al. [10, 24] performed research on heat transfer in smooth and ribbed 2:1 rotating channels at high rotation number up to 0.45 with a sudden expansion entrance which is same as the configuration in the current study.

The level of heat transfer enhancement in the two pass channel with angled ribs is also altered by rotation and by rotation-induced buoyancy forces. Figure 5 shows the secondary flows induced by rotation and angled ribs with a channel orientation of 135°. In Figure 5 (a), the Coriolis force induces a pair of vortices, favoring the trailing-outer corner in the first pass and leading-outer corner in the second pass. In Figure 5 (b), the pair of vortices induced by 45° parallel ribs

has the same flow direction as those due to rotation near leading and trailing surfaces in the second pass and reversed in the first pass. When the mainstream flow passes through the 180° turn, the flow impinges on the tip cap, then attaches to the outer wall right after the turn in the second pass, then reattaches on the inner wall as shown in Figure 4. A circulation zone right after the turn near the inner wall in the second pass is created due to flow separation. Two additional circulation zones occur in the outer corners of the turn because of the geometry and corresponding characteristic flow. The combination of these complex flow behaviors may result in enhancement of the heat transfer, or they may have a negative impact on the heat transfer trend. The flow patterns previously described have been observed by previous studies (Liou and Chen [28], Son et al. [29], Dutta et al. [30], Schabacker et al. [31]).

Rotation causes a difference in the heat transfer. The effect of rotation is evaluated by the rotation number (*Ro*), defined as the ratio of the Coriolis force to the inertial force as shown in Eq. (4).

$$Ro=(\Omega D_h)/U_b \quad (4)$$

The combined effect of rotation and coolant temperature gradient is evaluated by the local buoyancy parameter (Bo_x). For heated channels, the inertial force is in the same direction as the centrifugal force in the first pass with radially outward flow and in the opposite direction in the second pass with radially inward flow. The local buoyancy parameter is defined in Eq. (5).

$$Bo_x=(\Delta\rho/\rho_{b,x})(Ro)^2(R_x/D_h) \quad (5)$$

This local buoyancy parameter can be re-written by incorporating the measured wall and bulk air temperatures as shown in Eq. (6).

$$Bo_x=[(T_{w,x}-T_{b,x})/T_{w,x}](Ro)^2(R_x/D_h) \quad (6)$$

The corresponding rotation number *Ro* and channel-averaged buoyancy parameter *Bo* at each tested Reynolds number and rotational speed are shown in Figure 6. To more accurately determine the local buoyancy parameter, the local wall temperature in the denominator of Eq. (6) is replaced by the local film temperature ($T_{f,x}$), which is the average of the local wall and the local bulk temperatures as shown in Eq. (7).

$$T_{f,x}=(T_{w,x}+T_{b,x})/2 \quad (7)$$

In current study, the highest rotation number of 0.45 is achieved at Reynolds numbers of 10,000 and rotation speed 400 rpm. Accordingly, the maximum local buoyancy parameter is obtained based on the highest *Ro* of 0.45 and an inlet density ratio of 0.11.

STREAMWISE Nu RATIO DISTRIBUTION RESULTS - STATIONARY

When the channel is not rotating, the flow complexity is reduced because of the absence of the Coriolis and rotational buoyancy forces and the rib effects previously stated as mainstream flow separation, recirculation and reattachment, turbulent mixing, and angled rib-induced secondary flow still exist.

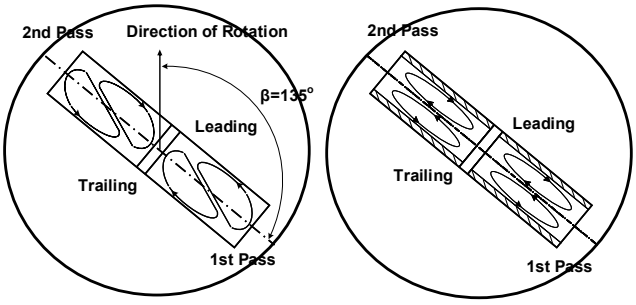

(a) (b)

Fig. 5 Conceptual secondary vortices induced by (a) rotation and (b) angled ribs

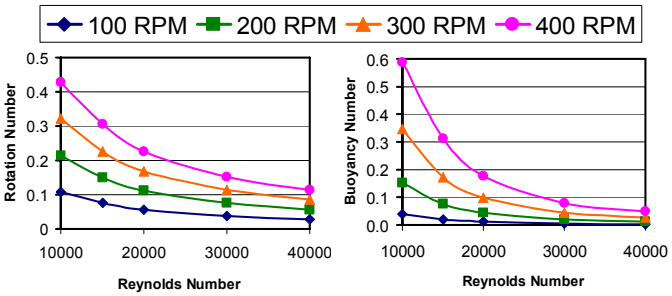

(a) (b)

Fig. 6 (a) Rotation number and (b) Buoyancy parameter at different Reynolds numbers and rotational speeds

The Nusselt ratio distributions of smooth and ribbed cases in the stationary channel at *Re*=20,000 and 40,000 are shown in Figure 7. For the smooth case, in the first passage, Nus/Nu_o ratio presents a characteristic trend of decreasing due to entrance effect on all walls. In the turn region (#6 & #7), heat transfer elevates prominently on trailing, leading and outer walls as observed by Son et al. [29]. In the second passage, Nus/Nu_o ratio decreases on leading and trailing walls and it reduces at a higher rate on outer wall, however, on the inner wall, Nus/Nu_o ratio remains a constant low value due to flow separation bubble along the divider wall and increases near exit.

For the ribbed cases, on leading, trailing and inner walls, the Nu_s/Nu_o ratio experiences a decrease and increase in the first and second passages, however, heat transfer drops substantially in the turn portion on leading and trailing walls. On the outer wall, the Nu_s/Nu_o ratio presents a similar trend as the smooth case in the first pass and obtains its maximum in the second pass. The decrease of heat transfer in the first/second passage on leading and trailing walls, similarly, is due to the entrance effect and the next increase is attributed to the angled rib-induced secondary flow. The heat transfer in the turn portion is largely decreased because most area in copper plate #6 and #7 is absent of ribs shown in Figure 4. The relatively low heat transfer on the outer wall compared to inner in the first pass and opposite trend in the second is due to the angle of

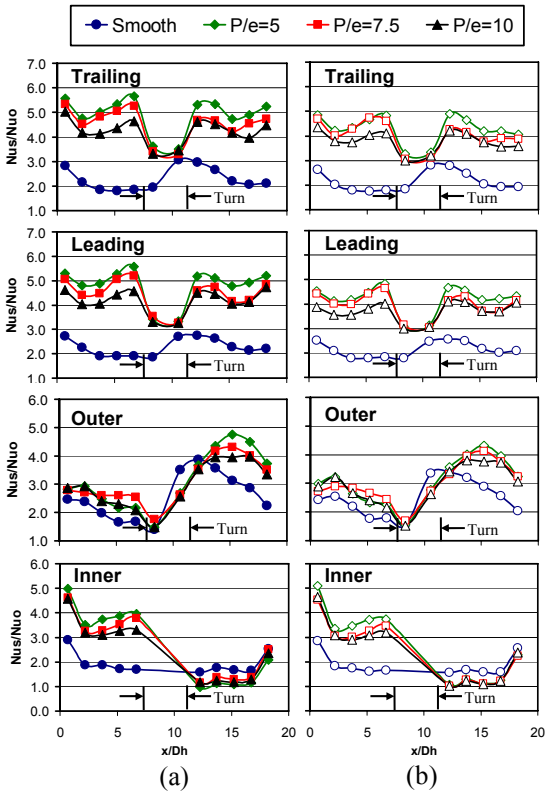

Fig. 7 Stationary streamwise *Nu* ratio (Nu_s/Nu_o) distribution at (a) *Re*=20,000 (b) *Re*=40,000

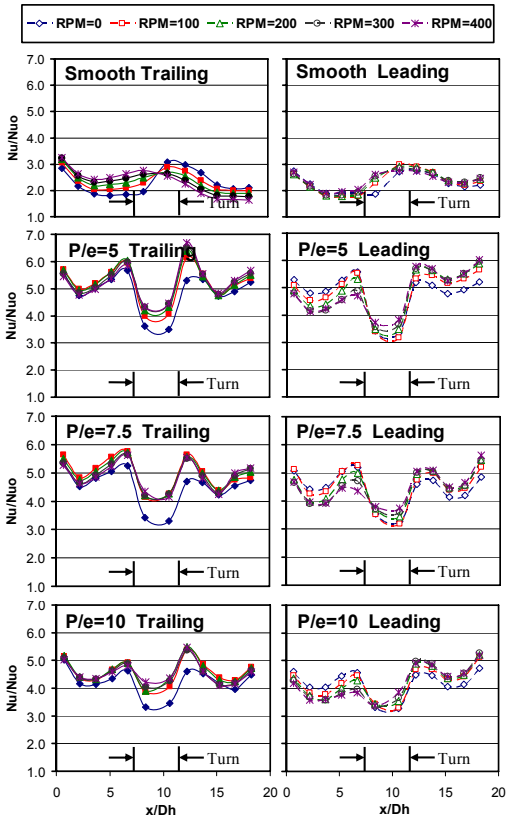

Fig. 8 Streamwise *Nu* ratio (Nu/Nu_o) distribution on the trailing and leading walls at *Re*=20,000

ribs, by which, relatively cold mainstream flow moves from the inner wall and impinges on outer as warm fluid in the first pass and vise versa. In the first or second passage, the effect of rib spacing (*P/e*) is obvious on leading and trailing surfaces as well as inner and outer walls, however, in the turn portion it is not significant. The Nu_s/Nu_o ratio increases as *P/e* ratio decreases in the passages due to the enhanced angled rib-induced secondary flows, but, in the turn portion, because of the partial coverage of ribs, the Nu_s/Nu_o ratio drops to the same low level for all *P/e* ratios. The effect of Reynolds number on Nusselt number ratio is observed between (a) and (b) of Figure 7. The Nu_s/Nu_o ratio on all surfaces in the channel decreases slightly with increasing Reynolds number. This can be explained as that the increase of Nu_s is not as much as the increase of Nu_o, which is determined by the Dittus-Boelter/McAdams correlation.

STREAMWISE Nu RATIO DISTRIBUTION RESULTS - ROTATING

The effects of rotation on streamwise Nu/Nu_o ratio distribution for leading and trailing walls with all *P/e* ratios and smooth cases at a Reynolds number of 20,000 are presented in Figure 8. For the smooth case, on the trailing surface, the Nu/Nu_o ratio increases with increasing rotation speed in the first pass and decreases in the second pass. However, on the leading surface, the Nu/Nu_o ratio is not as sensitive to rotation speed as that on the trailing surface in the whole channel. The heat transfer behavior of the trailing surface is mostly due to the Coriolis force which pushes mainstream toward trailing in the first pass and leading in the second pass. Rotational buoyancy also helps the trailing surface in the first pass due to the additional near-wall turbulence. For the ribbed cases, on the trailing surfaces, the Nu/Nu_o ratio presents a streamwise distribution similar to the stationary case, except for the area near turn portion (copper plates #5, #6, #7, and #8), where heat transfer level increases 25% approximately. Obviously, the ribs reduce the effect of rotation in the first and second passage. The variation of the Nu/Nu_o ratio for different rotation speeds (*RPM*=100, 200, 300, and 400) is reduced in the whole channel. Comparatively, on the leading surface, except for the similar trend of streamwise distribution as trailing, Nu/Nu_o ratio decreases with higher rotation speed in the first pass and increases in the second pass, in which a larger effect of rotation is observed comparing to the smooth case. The effect of *P/e* ratios on heat transfer in the rotating channel plays a role similar to that in the stationary channel on leading and trailing walls. The Nu/Nu_o ratio increases with decreasing *P/e* ratio in the whole channel except for the turning portion where Nu/Nu_o ratio keeps the same level.

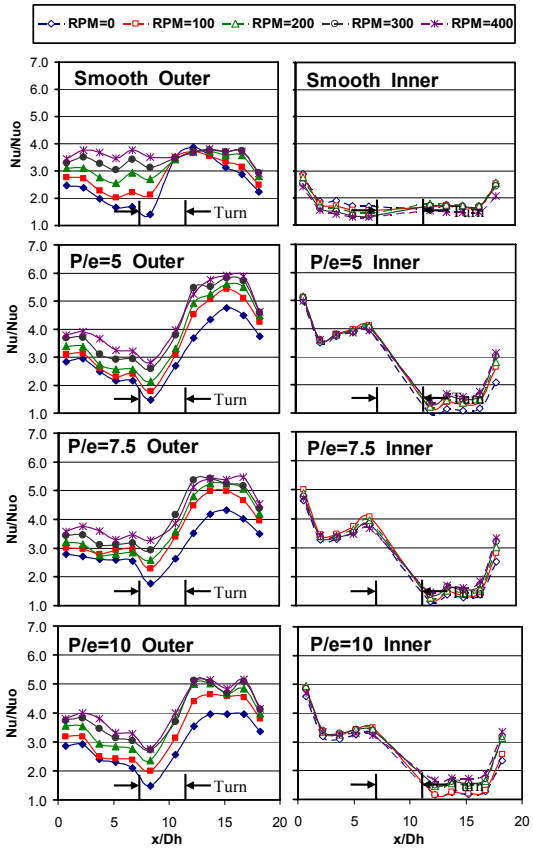

Fig. 9 Streamwise *Nu* ratio (Nu/Nu_o) distribution on the outer and inner walls at *Re*=20,000

The effects of rotation on streamwise Nu/Nu_o ratio distribution for outer and inner walls are shown in Figure 9. For the smooth case, on the outer wall, the Nu/Nu_o ratio is increased with increasing rotation speed in both passages and in the first pass a larger effect of rotation is shown. Contrarily, an opposite trend is observed on the inner wall that Nu/Nu_o ratio is decreased with increasing rotation speed in both passes. For the present passage orientation of 135° shown in Figure 5, the change of heat transfer due to rotation on the outer and the inner surface is analogous to that on the trailing and the leading wall where the cold mainstream flow favors the former because of the Coriolis force. For the ribbed cases, on the outer wall, the Nu/Nu_o ratio variation due to different rotation speeds is slightly reduced in the first pass and greatly increased in the second pass comparing with the smooth case, which is attributed to the combined effect of rotation and the angled ribs. The effect of *P/e* ratios is to slightly decrease Nu/Nu_o on inner wall of the first passage and outer wall of the second passage when reducing *P/e*. On the first pass outer wall and the second pass inner wall, Nu/Nu_o is not sensitive to *P/e* ratios. It is noted that the Nu/Nu_o ratios are relatively low on the second pass inner wall. This is possibly due to the separation bubble on the divider wall induced by the 180° sharp turn.

EFFECT OF ROTATION NUMBER

The rotation number (*Ro*) as defined in Eq. (4) is used to describe the ratio of the Coriolis force to the bulk inertial force and can be reached by various combinations of rotational speed and mainstream flow velocity. The rotation number in this study varies from 0 to 0.45. In Figure 10 the effect of rotation on heat transfer (Nu/Nu_s) is presented as a function of the rotation number at region #4 and #9, where the combined effects of the entrance/exit and the turn are expected to be at minimum. The stationary Nusselt number (Nu_s) is chosen as the denominator so that the effects of rotation can be compared.

For the smooth case, in the first passage, the *Nu/Nus* ratio increases substantially with higher *Ro* on the trailing and the outer surface, and decreases greatly on the inner wall. However, on the leading wall, Nu/Nu_s ratio experiences a minimum at low *Ro* and then increases to a value above 1. In the second passage, the Nu/Nu_s ratio's variation is limited around unit on the leading surface and a steep decrease of Nu/Nu_s is observed on the trailing wall. Besides, on outer and inner surfaces, the behavior of Nu/Nu_s is similar to that in the first passage, however, in a reduced range. For the current channel with 135° orientation angle, in the first pass with radially outward flow, the Coriolis force skews the bulk flow towards the trailing and outer wall, which attributes to the Nu/Nu_s values above 1.0 on trailing and outer walls as well as the Nu/Nu_s values below 1.0 on leading and inner walls. In the second pass, the combined effects of the secondary flows induced by the 180° turn and rotation determine the Nu/Nu_s ratio variation in the second passage.

For the ribbed cases, in the first passage, the Nu/Nu_s ratio experiences slight variations around 1.0 on the trailing wall and it decreases a lot and then increases slightly on the leading surface. On the outer wall, the Nu/Nu_s ratio increases monotonously to a value smaller than smooth case. On the inner wall it starts to decrease at a higher *Ro*, comparing with the smooth case. In the second passage, on both leading and trailing surfaces, the Nu/Nu_s ratio elevates above 1.0 and the increase of heat transfer on the leading surface is about 10% higher than the trailing surface. On the outer wall, similar to the smooth case, the Nu/Nu_s ratio keeps increasing with *Ro*, however, on the inner wall, an increase of heat transfer is observed, which is opposite to the smooth data. In Figure 5, it is obvious that in the first passage, near the trailing surface, the secondary flow induced by ribs is in the opposite direction to that by rotation, thus the effect of rotation is reduced and the heat transfer enhancement is surpressed. For outer and inner walls, similar to stationary cases, the rib inducts the relatively cool air from inner to outer and during the process air is heated continuously. Thus, ribs weaken the heat transfer on the outer wall and strengthen it on the inner wall, which is counteracting to the Coriolis effects by rotation. In the second passage, near the leading surface, the secondary flow induced by ribs is in the same direction as that by rotation, thus the effect of rotation is increased and the heat transfer enhancement is increased as much as 15%. However, near the trailing surface, the relatively

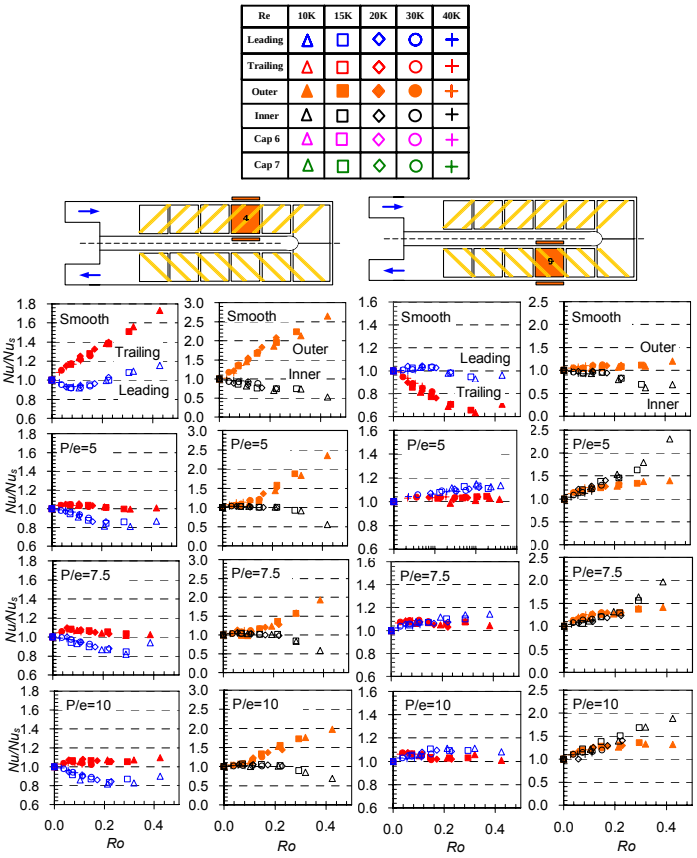

Fig. 10 Nu/Nu_s distribution vs rotation number on all surfaces at region #4 & 9

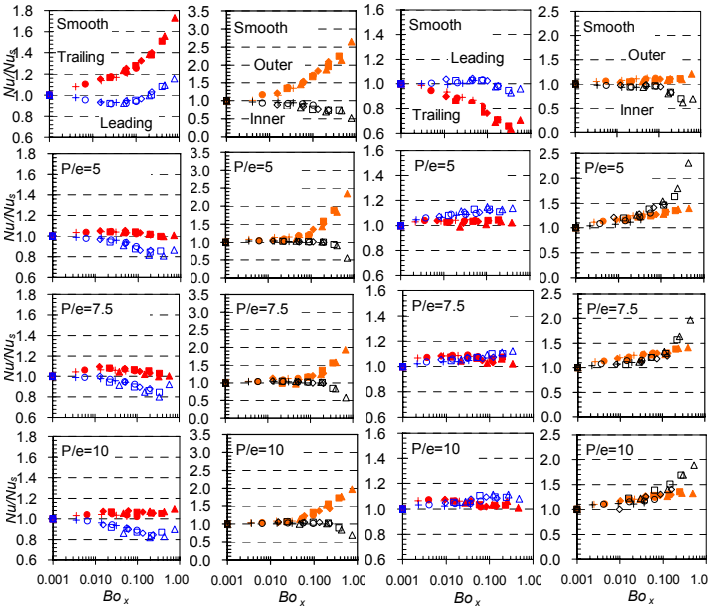

Fig. 11 Nu/Nu_s distribution vs local buoyancy parameter on all surfaces at region #4 & 9

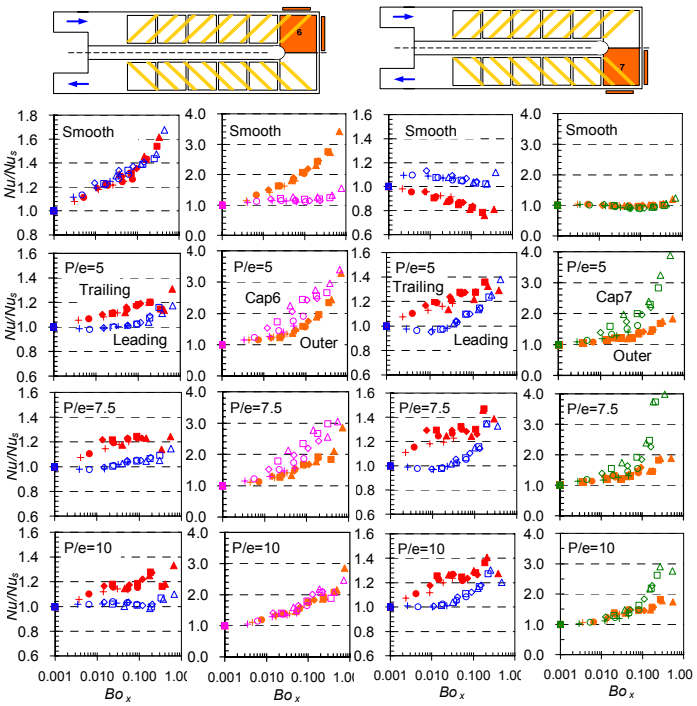

Fig. 12 Nu/Nu_s distribution vs local buoyancy parameter in the 180° turn portion at region 6 & 7

thick boundary layer is largely reduced and as a result, the heat transfer on the trailing surface is slightly increasing. For outer and inner walls, the heat transfer is largely affected by the strong turn-induced secondary flows, Coriolis force and the ribs. The effect of different P/e ratios on Nu/Nu_s is not very obviously shown in Figure 10, in that the Nu_s in the denominator has already considered the heat transfer difference by P/e ratios.

EFFECT OF BUOYANCY PARAMETER

When the walls of the test section are heated, a temperature profile is developed in the fluid from mainstream core to wall surfaces. The temperature profile produces a variation of fluid density in the channel. The density variation and centrifugal force by rotation result in the rotation-induced buoyancy force that drives the hotter and lighter fluid near the heated surface toward the center of rotation. The combined effects of density difference and rotation on heater transfer are presented by studying the Nu/Nu_s ratios vary with the change of buoyancy parameter. In Figure 11 and 12, the effects of the local buoyancy parameter (Bo_x) on Nu/Nu_s ratios are shown on all surfaces of section 4, 6, 7, and 9.

The effects of the local buoyancy parameter (Bo_x) on Nu/Nu_s ratios in the first and second passages are shown in Figure 11. The trend of Nu/Nu_s with respect to Bo_x is very similar to that to Ro discussed in last section in that inlet density ratio keeps the value of 0.11 and effects of density ratio ($\Delta\rho/\rho_{b,x}$) on Nu/Nu_s can not be shown. At region #4 of the

smooth channel, the most prominent phenomenon occurs at the leading surface where the Nu/Nu_s ratio experiences a slight drop and then an elevation. It can be explained as the flow stagnation and separation near the surface due to opposite directions of buoyancy force and bulk flow.

For the ribbed cases, at region #4 & #9, the Nu/Nu_s ratios variations follow the trend of Nu/Nu_s to Ro in Figure 10 respectively but in a different x-axis scale. Considering the three P/e ratios, on all surfaces, the Nu/Nu_s ratios are not very sensitive to P/e.

The effects of Bo_x on Nu/Nu_s ratios at region #6 and #7 in the turn portion are shown in Figure 12. For the smooth cases, at region #6, the Nu/Nu_s ratio experiences substantial increase on leading, trailing and outer walls but it elevates slightly at large Bo_x on the cap surface. At region #7, the Nu/Nu_s ratio behaves totally differently where it increases little on leading, outer and cap walls and it decreases on the trailing surface. For the ribbed channels, at region #6, the Nu/Nu_s ratio elevates on all walls when Bo_x increases and it is obvious that ribs weaken the effect of buoyancy on leading and trailing walls while they strengthen the buoyancy effect on the cap. At region #7, similar trend of Nu/Nu_s with Bo_x is observed on all surfaces as that at region #6. The effects of different P/e ratios on Nu/Nu_s are very similar to each other, except that on outer and cap walls Nu/Nu_s decreases slightly with higher P/e ratio at both region #6 and #7.

CONCLUSION

This research studied the effect of rib pitch-to-height ratios (P/e=5, 7.5 and 10) in a 2:1 aspect ratio rotating channel with a realistic orientation angle of 135°. Based on the result, the following conclusions have been made:

1. For the stationary cases (Re=10,000 to 40,000), the streamwise Nu_s/Nu_o ratios increase with decreasing rib pitch-to-height ratios (P/e=10, 7.5 and 5) on trailing and leading surfaces and larger Re produces smaller Nu_s/Nu_o ratio on all surfaces.
2. For the large rotation numbers or buoyancy parameters, the streamwise Nu_s/Nu_o ratios are greatly affected on all surfaces in the smooth and ribbed channels.
3. The effect of rotation on heat transfer is largely decreased by applying ribs on leading and trailing surfaces for this 2:1 aspect ratio channel. The substantial variations of Nu/Nu_s on the leading or trailing surface due to rotation are reduced, and the maximum variation remains in the range of +/-20% for ribbed cases.
4. The effect of rib pitch-to-height ratios (P/e=5, 7.5 and 10) on the Nu/Nu_s ratio is small under rotation conditions.
5. The effect of rotation on heat transfer on outer and inner surfaces is slightly decreased by ribs in the first pass. In the second pass, the effect of rotation is tremendously increased on the inner surface due to the combined effects of ribs, rotation and 180° turn induced secondary flows.
6. In the turn portion, for both smooth and ribbed channels, the effect of rotation is to increase heat transfer on tip cap and outer surfaces substantially (except at region #7 of the smooth channel, heat transfer increases 20% at highest rotation number (Ro)) and in this portion, both leading and trailing surfaces experience whole-scale heat transfer increase as local buoyancy parameter increases.
7. Nu/Nu_s ratios can be correlated by rotation number (Ro) or buoyancy parameter (Bo) on all surfaces in the smooth and the ribbed channels.

ACKNOWLEDGMENTS

The project was sponsored by the Marcus C. Easterling Chair endowment funds.

REFERENCES

[1]Han, J.C., Dutta, S., Ekkad, S.V., 2000, Gas Turbine Heat Transfer and Cooling Technology, Taylor and Francis, New York

[2]Han, J.C., 1988, "Heat Transfer and Friction Characteristics in Rectangular Channels with Rib Turbulators", ASME J. Heat Transfer, Vol. 110, pp. 321-328.

[3]Han, J.C. and Park, J.S., 1988, "Developing Heat Transfer in Rectangular Channels with Rib Turbulators", Int. J. of Heat Mass Transfer, Vol. 31, pp. 183-195.

[4]Park, J.S., Han, J.C., Huang, Y., Ou, S., 1992, Heat Transfer Performance Comparisons of Five Different Rectangular Channels with Parallel Angled Ribs", Int. J. of Heat Mass Transfer, Vol. 35, No. 11, pp. 2891-2903.

[5]Han, J.C., Glicksman L.R., Rohsenow, W.M., 1978, "An Investigation of Heat Transfer and Friction for Rib-Roughened Surfaces", Int. J. Heat Mass Transfer, Vol. 21, pp. 1143-1156.

[6]Taslim, M.E., Spring, S.D., 1994, "Effects of Turbulator Profile and Spacing on Heat Transfer and Friction in a Channel", J Thermophysics Heat Transfer, Vol. 8, pp.555-562.

[7]Wagner, J.H., Johnson, B.V., Hajek, T.J., 1991a, "Heat Transfer in Rotating Passages with Smooth Walls and Radial Outward Flow", ASME J. Turbomachinery, Vol. 113, pp. 42-51.

[8]Wagner, J.H., Johnson, B.V., Kooper, F.C., 1991b, "Heat Transfer in Rotating Passage with Smooth Walls", ASME J. Turbomachinery, Vol. 113, pp. 321-330.

[9]Han, J.C., Zhang, Y.M., Kalkuehler, K., 1993, "Uneven Wall Temperature Effect on Local Heat Transfer in a Rotating Two-Pass Square Channel with Smooth Walls", ASME J. Heat Transfer, Vol. 115, pp. 912-920.

[10]Huh, M., Lei, J., Liu, Y.H., and Han, J.C., 2009, "High Rotation Number Effects on Heat Transfer in a Rectangular (AR=2:1) Two-Pass Channel", ASME Paper No. GT2009-59421.

[11]Wagner, J.H., Johnson, B.V., Graziana, R.A., and Yeh, F.C., 1992, "Heat Transfer in Rotating Serpentine Passages with Trips Normal to the Flow", ASME J. Turbomachinery, Vol. 114, pp. 847-857.

[12]Johnson, B.V., Wagner, J.H., Steuber, J.D., and Yeh, F.C., 1994, "Heat Transfer in Rotating Serpentine Passages with

Trips Skew to the Flow", ASME J. Turbomachinery, Vol. 116, pp. 113-123.
[13]Taslim, M.E., , Bondi, L.A., Kercher, D.M., 1991, "An Experimental Investigation of Heat Transfer in an Orthogonally Rotating Channel Roughened With 45 deg Criss-Cross Ribs on Two Opposite Walls", ASME J. Turbomachinery, Vol. 113, pp. 346-353.
[14]Fu, W.L., Wright, L.M., Han, J.C., 2004, "Heat Transfer in Two-Pass Rotating Rectangular Channels (AR=1:2 and AR=1:4) with 45^o Angled Rib Turbulators", ASME Paper No. GT 2004-53261.
[15]Fu, W.L., Wright, L.M., Han, J.C., 2005, "Buoyancy Effects on Heat Transfer in Five Different Aspect-Ratio Rectangular Channels with Smooth Walls and 45-Degree Ribbed Walls", ASME Paper No. GT 2005-68493.
[16]Su, G., Chen, H.C., Han, J.C., Heidmann, D., 2004, "Computation of Flow and Heat Transfer in Two-Pass Rotating Rectangular Channels (AR=1:1, AR=1:2, AR=1:4) with 45-Deg Angled Ribs by a Reynolds Stress Turbulence Model", ASME Paper No. GT2004-53662.
[17]Liu, Y.H., Wright, L.M., Fu, W.L., and Han, J.C., 2006, "Rib Spacing Effect on Heat Transfer and Pressure Loss in a Rotating Two-Pass Rectangular Channel (AR=1:2) with 45-Degree Angled Ribs", ASME Paper No. GT2006-90368.
[18]Huh, M., Liu, Y.H., Han, J.C., 2009, "Rib-Spacing Effect on heat Transfer in Rectangular Channels at High Rotation Numbers", AIAA J. Thermophysics and Heat Transfer, Vol. 23, pp. 294-304.
[19]Johnson, B.V., Wagner, J.H., Steuber, G.D., and Yeh, F.C., 1994, "Heat Transfer in Rotating Serpentine Passages with Selected Model Orientations for Smooth or Skewed Trip Walls", ASME J. Turbomachinery, Vol. 116, pp. 738-744.
[20]Parsons, J.A., Han, J.C., Zhang, Y., 1995, "Effect of Model Orientation and Wall Heating Condition on Local Heat Transfer in a Rotating Two-Pass Square Channel with rib turbulators", Int. J. Heat Mass Transfer, Vol. 38, pp. 1151-1159.
[21]Dutta, S. and Han, J.C., 1996, "Local Heat Transfer in Rotating Smooth and Ribbed Two-Pass Square Channels with Three Channel Orientations", ASME J. Heat Transfer, Vol. 118, pp. 578-584.
[22]Azad, G.S., Uddin, M.J., Han, J.C., Moon, H.K., and Glezer, B., 2002, "Heat Transfer in a Two-Pass Rectangular Rotating Channel with 45-deg Angled Rib Turbulators", ASME J. Turbomachinery, Vol. 124, pp. 251-259.
[23]AL-Hadhrami, L.M., Griffith, T.S., Han, J.C., 2002, "Heat Transfer in Two-Pass Rotating Rectangular Channels (AR=2) with Parallel and Crossed 45o V-shaped Rib Turbulators", AIAA Paper No. A02-13915.
[24]Huh, M., Lei, J., Han, J.C., 2010, "Influence of Channel Orientation on Heat Transfer in a Two-Pass Smooth and Ribbed Rectangular Channel (AR=2:1) under Large Rotation Numbers", ASME Paper No. GT2010-22190.
[25]Kline, S.J., McClintock, F.A., 1953, "Describing Uncertainty in Single-Simple Experiments", Mechanical Engineering, Vol. 75, pp. 3-8.
[26]Wright, L.M., Fu, W.L., Han, J.C., 2005, "Influence of Entrance Geometry on Heat Transfer in Rotating Rectangular Cooling Channels (AR=4:1) with Angled Ribs", ASME J. Heat Transfer, Vol. 127, pp. 378-387.
[27]Liu, Y.H., Huh, M., Han, J.C., Chopra, S., 2007, "Heat Transfer in a Two-Pass Rectangular Channel (1:4) Under High Rotation Numbers", ASME Paper No. GT2007-27067.
[28]Liou, T.M., Chen, C.C., 1999a, "LDV Study of Developing Flows through a Smooth Duct with a 180 Deg Straight-Corner Turn", ASME J. Turbomachinery, Vol. 121, pp.167-174
[29]Son, S., Kihm, K.D., Han, J.C., 2002, "PIV Flow Measurements for Heat Transfer Characterization in Two-Pass Square Channels with Smooth and 90^o Ribbed Walls", Int. J. Heat Mass Transfer, Vol. 45, pp. 4809-4822.
[30]Dutta, S., Andrews, M., Han, J.C., 1996, "Prediction of Turbulent Heat Transfer in Rotating Smooth Square Ducts", Int. J. Heat Mass Transfer, Vol. 39, No. 12, pp. 2505-251.
[31]Schabacker, J., Bolcs, A., Johnson, B.V., 1998, "PIV Investigation of the Flow Characteristics in an Internal Coolant Passage with Two Ducts Connected by a Sharp 180^o Bend", ASME Paper No. 98-GT-544.